J. Plasma Fusion Res. SERIES, Vol. 3 (2000) 580–583

# Theoretical Analysis of Transport Barriers in Helical Systems

TODA Shinichiro and ITOH Kimitaka
*National Institute for Fusion Science, Toki-shi, Gifu, 509-5292, JAPAN*

(Received: 18 January 2000 /Accepted: 17 April 2000)

**Abstract**

A set of one-dimensional model equation in helical system is analyzed including the electric field bifurcation. The spatial and temporal evolutions of the temperature and the electric field are examined. A spatial structure which is related with the edge transport barrier is duscussed. A self-generated oscillation of the edge temperature and the heat flux loss takes place under the constant heat flux from the core. The oscillation occurs near the transition boundary. The transport barrier in the inner region is found in the high confinement state.

**Keywords:**
helical system, transport barrier, transition, self-generated oscillation

## 1. Introduction

The reduction of anomalous transport has been analyzed in the Heliotron configuration based on the turbulent transport model [1] and the internal transport barrier has been studied in helical plasmas due to the electric field bifurcation [2]. Steep gradient of the radial electric field and the internal transport barrier have been found in the CHS plasma recently [3]. Through these theoretical and experimental studies, the possibility of the internal transport barrier has been explored. In these previous theoretical studies, the critical heat flux was obtained for the transition based on zero-dimensional model [2]. The investigation about the dynamics and the spatial structure is needed in consideration with the spatial dependence of the physical quantities.

In this article, the model associated with the transport barrier in helical system is presented. The possibility for the transport barriers (the edge transport barrier and the internal transport barrier) based on the bifurcation model of the electric field is discussed. We examine a set of one-dimensional transport equations which constitute the temporal evolution of the temperature and the diffusion of the radial electric field. The simplified form [2] of the neoclassical flux which is associated with the helical-ripple trapped particles is used. We study about the radial dependence of the temperature and the heat conductivity and show the states which relate the transport barriers.

## 2. One-dimensional Model Equations

In this section, we show the model equations used here. We use cartesian coordinates and the x-axis is taken in the radial slab plasma in this article. We consider the slab region $0 \le x \le a$, where $a$ is the minor radius. We here use quasi-neutrality $n = n_e = n_i$. The neoclassical flux associated with the helical-ripple trapped particles are discussed in [4] and is simplified as

$$\Gamma_e = \frac{n}{a} D_e \left( -a\frac{n'}{n} - \frac{eaE_r}{T_e} - \eta_{12}\frac{aT_e'}{T_e} \right) \qquad (1)$$

and

*Corresponding author's e-mail: toda@tadws25.nifs.ac.jp*

$$\Gamma_i = \frac{n}{a} D_i \frac{1}{1 + C_i (eaE_r / T_e)^2} \left( -a\frac{n'}{n} + \frac{T_e}{T_i} \frac{eaE_r}{T_e} \right), \quad (2)$$

where the coefficient $\eta_{12}$ are a numerical constant of order unity, $C_j = 1.5(\varepsilon_t/\varepsilon_h)^{1/2}(T_e/(\nu_j r B e a))^2$ and the diffusivity $D_j = C\varepsilon_t^2 \varepsilon_h^{1/3} v_D^2/\nu_j$ for the species $j$. Here, $\varepsilon_t$ is the toroidal aspect ratio, $\varepsilon_h$ is the helical ripple, $\nu_j$ is the collision frequency, $v_D$ is the toroidal drift velocity and $T_j$ is the temperature. The prime denotes the derivative with respect to the radial direction. We set the normalized parameters; $X = \sqrt{C_i} eaE_r/T_e$, $N = -\sqrt{C_i} an'/n$ and $Y = -\sqrt{C_i}\eta_{22} aT_e'/T_e$. We here take a limit of a strong electron temperature gradient. For example, this is suitable for the case of electron cyclotron heating where the density profile is often observed to be flat. For this case, the energy flow in the electron channel is larger than that in ion channel. Using these normalized variables and if we may take a limit of a strong electron temperature gradient, $|T'/T| >> |n'/n|$, Eqs. (1) and (2) are simplified as $\hat{\Gamma}_e = -X + bY$ and $\hat{\Gamma}_i = \xi\zeta X/(1 + X^2)$, where $b = \eta_{12}/\eta_{22}$, $\xi = D_i/D_e$, $\zeta = T_e/T_i$, $\hat{\Gamma}_e = \sqrt{C_i} a\Gamma_e/(nD_e)$ and $\hat{\Gamma}_i = \sqrt{C_i} a\Gamma_i/(nD_e)$. The parameter $\eta_{22}$ is the coefficient related with the gradient of $T_e$ in the formula for the heat flux of electrons. We omit the subscript $e$ with respect to the temperature, $T = T_e$, in the following description.

Under the assumption that the density is constant temporally and spatially, the temporal evolution of temperature $T$ is written as

$$\frac{\partial T}{\partial t} = \frac{\partial}{\partial x} \left( \chi(X) \frac{\partial T}{\partial x} \right), \quad (3)$$

where the normalizations $t/\tau_E \to t$, $x/a \to x$, $\chi/\chi_0 \to \chi$, $T/T_0 \to T$. The subscript 0 represents the typical value of the physical quantity and $\tau_E = (a^2/\chi_0)$ is the energy confinement time. The modelled heat conductivity $\chi(X)$ is given as $\chi = \chi_{NC0}/(1 + X^2) + \chi_{anom}$. The first term in the right hand side represents the component which depends on the radial electric field (*e.g.*, in some limit, of neoclassical heat conductivity) and the second term is the component which is independent of the radial electric field (*e.g.*, in some limit, anomalous one), respectively. In Sec. 3, we study the both cases taking only the part which depends on the electric field and only the part of the heat conductivity which is independent of the electric field. In Sec. 4, we take only the part which depends on the electric field of the heat conductivity. Here, the heat source is neglected in the region considered here and the heat flux is given as a boundary condition. The equation for the time evolution of the radial electric field $E_r$ is shown as

$$\varepsilon \frac{\partial X}{\partial t} = \hat{\Gamma}_e - \hat{\Gamma}_i + \mu \frac{\partial^2 X}{\partial x^2}. \quad (4)$$

Here, $\mu$ is the normalized shear viscosity of ions. The parameter $\varepsilon$ is given by $\varepsilon = \tau_r/\tau_E$, where the parameter $\tau_r (= \tau_E(\varepsilon_\perp T/(e^2 n a^2)))$ is the typical time in which the radial electric field changes. The parameter $\varepsilon_\perp$ ($\simeq (1 + 2q^2)\varepsilon_0 c^2/v_A^2$) is the perpendicular dielectric constant for a magnetized plasma, $\varepsilon_0$ is the dielectric constant in the vacuum, $q$ is the safety factor, $c$ is the light speed and $v_A$ is the Alfvén velocity in the plasma. For parameters $B = 1$ $(T)$, $T = 300$ $(eV)$ and $a = 0.2$ $(m)$, we obtain $\tau_r/\tau_E \simeq 0.01$. When the quantities of temperature and density are specified in Eq. (4), the location of the electric field interface has been determined according to the Maxwell's construction [2].

## 3. Stationary State and Transport Barrier

In this section, we fix $q_{in} = 10$, where $q_{in}$ is the heat flux $q$ $(= -\chi\nabla T)$ at $x = 0$. We set $-T'/T = 10$ at the edge $(x = 1)$ to examine the solution of the high confinement. Furthermore, we choose $X'' = 0$ at $x = 0$ and $x = 1$ to study the structure of the electric domain.

At first, we choose the part which depends on the electric field; $\chi = \chi_{NC0}/(1 + X^2)$ for the heat conductivity. The cases for two values ($\mu = 1$ and $\mu = 1 \times 10^{-2}$) of the ion viscosity are studied. The parameters are shown as $\varepsilon = 0.01$, $\chi = \chi_{NC0} = 1$, $b = 1$, $\xi = 1$ and $\zeta = 16.0$. Stationary temperature profiles are shown in Fig. 1(a), analyzing Eqs. (3) and (4). The spatial structures of the radial electric field $X$ are also given in Fig. 1(b). The steep gradient is obtained and the transport barrier with the some radial width near the edge is seen in both cases. The radial width of the transport barrier is found to be proportional to $\sqrt{\mu}$, which is the same dependence

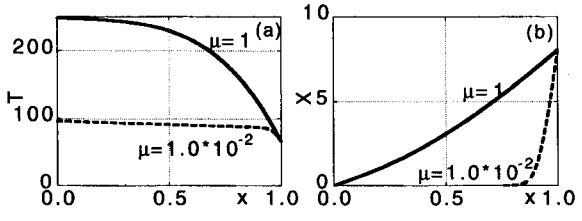


Fig. 1 The radial dependence of the stationary (a) temperature and (b) radial electric field two cases, $\mu = 1$ and $\mu = 1 \times 10^{-2}$. The model of the heat conductivity is $\chi = \chi_{NC0}/(1 + X^2)$.

with that in Ref. [5].

To examine the stationary results in details, we show the stationary solutions on ($Y$, $X$) plane in Fig. 2. The dotted line shows the ambipolar condition $\hat{\Gamma}_e = \hat{\Gamma}_i$ in Eq. (4). In the line of the ambipolar condition, the branch for the large $X$ is namely called as the high confinement mode (H-mode) because the flux is reduced for the larger $X$. On the contrary, the branch for the smaller $X$ is named as the low confinement mode (L-mode). The state around the upstream corresponds to the L-mode, while the state at the edge corresponds to the H-mode. The value of the diffusion term of $X$; $\mu\partial^2 X/\partial x^2$ is the contribution which balances with the deviation $X[Y]$ from the ambipolar condition. If the value of $\mu$ decreases, the line which represents the stationary state gets nearer to ambipolar condition (See Fig. 2) (but does not converge). This is because both Eq. (3) and the ambipolar condition do not necessarily hold at the same time in the stationary state.

Next, we employ only the part which is independent of the electric field $\chi = \chi_{anom}$ (= 1) for the heat conductivity. The boundary condition is same with the case with the heat conductivity $\chi = \chi_{NC0}/(1 + X^2)$ in this section. In this case, both the stationary solutions of Eq. (3) and the ambipolar condition can hold at same time, because Eq. (3) is not coupled with the variable $X$. Therefore, if the value of $\mu$ approaches to zero, the line which represents the stationary state gets near to the ambipolar condition in Fig. 3. If the value of $\mu$ is close to zero, the Maxwell's construction is confirmed to hold.

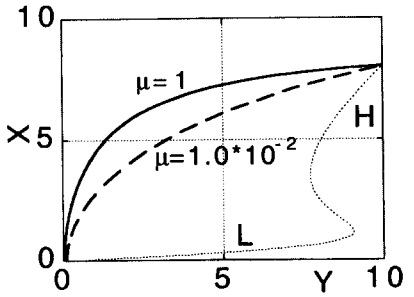


Fig. 2 The stationary dependence on $Y$-$X$ plane with the model $\chi = \chi_0/(1 + X^2)$.

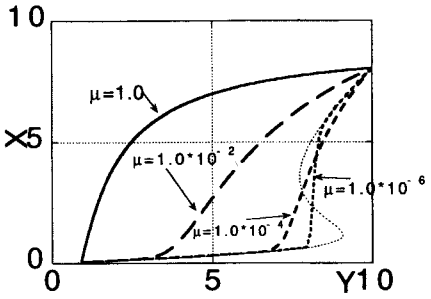


Fig. 3 The stationary dependence on $Y$-$X$ plane when the heat conductivity model $\chi = \chi_{anom}$ is used.

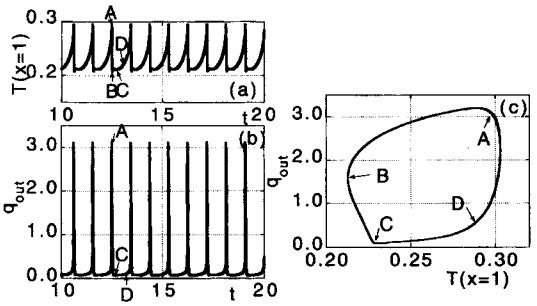


Fig. 4 The temporal evolutions of (a) the edge temperature, and (b) the heat flux at the edge $q_{out}$. The parameters are written in text. The trajectory in the $q_{out}$ – $T(x = 1)$ plane is shown in Fig. 4(c). The time sequence is indicated by *A*, *B*, *C* and *D* with arrows in (a), (b) and (c).

## 4. Periodic Oscillation and Transport Barrier

We choose $-T' = 2$ at the edge in this section. We again set $X'' = 0$ at $x = 0$ and $x = 1$ to study the interface between the low and high confinement states. We examine the calculation results for the various values of $q_{in}$. Next, we choose the heat conductivity $\chi = \chi_{NC0}/(1 + X^2)$. Solving Eqs. (3) and (4) with these boundary conditions, the periodic oscillations of the edge temperature $T(x = 1)$ and of the heat flux at the edge ($x = 1$) $q_{out}$ are obtained. In Fig. 4, we show the temporal evolutions of (a) the temperature at the edge, (b) the heat flux at the edge $q_{out}$ and (c) the Lissajous figure on the $q_{out}$ – $T(x = 1)$ plane. The parameters are same as those in Sec. 3, while $q_{in} = 0.2$ and $\mu = 1$. In the constant flux from upstream, the solution behavior is classified to three categories. If $q_{in}$ is smaller than 0.083 the lower flux solution is stationary, which corresponds to H-mode. In the region $0.083 < q_{in} < 1.54$, the limit cycle solution is obtained. The upper and lower boundary of $q_{in}$ value is determined by the gradient of the temperature at the edge. If $q_{in}$ becomes larger than 1.54, the higher flux solution becomes stationary.

In Figs. 5(a) and (b), temporal changes of the radial profiles of temperature and effective heat conductivity are shown. The heat conductivity becomes more

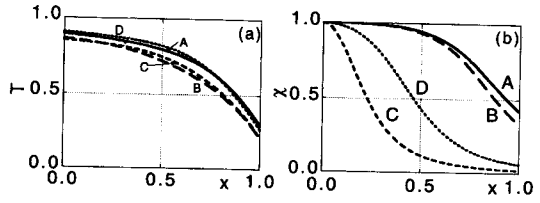


Fig. 5 The spatial structure of (a) temperature and (b) heat conductivity.

suppressed from the edge to the upstream side in H-mode state (case *C*) compared with that in L-mode (case *A*). A transport barrier with a finite extent is seen at $x \approx 0.3$ in the radial structure of $\chi$ in H-mode.The transition is found to propagate from the edge to the upstream side,judging from the points which hold the relation $dX/dt = 0$.

## 5. Summary and Discussions

In summary, the model equation of the electric field bifurcation is newly shown to contain the temporal and spatial evolutions of the plasma temperature and radial electric field. The formula of the particle flux in helical systems is included in the diffusion equation of the radial electric field *X*.

The stationary radial dependence of the temperature is examined for the various values of the shear viscosity $\mu$ of ions. The transport barrier at the edge is found. The qualitative change of the stationary state due to the models, i.e., $\chi = \chi_{NC0}/(1 + X^2)$ and $\chi = \chi_{anom}$ is also studied. Next, limit cycle solutions of the temperature and the heat flux are obtained in helical systems. It is found that the dependence of thermal conductivity on the electric field strongly influences on the location of the interface. This finding illustrates the importance of the one-dimensional analysis compared to zero-dimensional analysis.

In this article, two parts (one part depends on the electric field and another part is independent of the electric field) for the heat conductivity are not studied at the same time. The heat conductivity which includes the both parts may add the variety of the structure and temporal evolution of the physical quantities. Furthermore, the coupling of the density development is neglected for the transparency of arguments in this article. In general, the spatial-temporal development of the density is considered to be important. These are left for future work.

## Acknowledgements

This work is partly supported by Grant-in-Aid for Scientific Research of Ministry of Education, Science, Sports and Culture of Japan.

## References

[1] K. Itoh *et al.*, Plasma Phys. Control. Fusion **36**, 123 (1994).

[2] K. Itoh *et al.*, 26th EPS Conf. on Control. Fusion and Plasma Phys. 14 – 18 June 1999, Maastricht, The Netherlands 1309.

[3] A. Fujisawa *et al.*, Phys. Rev. Lett. **79**, 1054 (1997); A. Fujisawa *et al.*, Phys. Rev. Lett. **82**, 2669 (1999).

[4] L. M. Kovrizhnykh, Comments on Plasma Physics and Controlled Fusion **9**, 239 (1986).

[5] S. -I. Itoh *et al.*, Phy. Rev. Lett. **67**, 2485 (1991).